

# Liquid–Liquid(–Liquid) Equilibria in Ternary Systems of Water + Cyclohexylamine + Aromatic Hydrocarbon (Toluene or Propylbenzene) or Aliphatic Hydrocarbon (Heptane or Octane)

Mandy Klauck, Andreas Grenner, and Jürgen Schmelzer\*

Department of Chemical Engineering, Hochschule für Technik und Wirtschaft Dresden–University of Applied Sciences, Friedrich-List-Platz 1, 01069 Dresden, Germany

Liquid–liquid equilibria and liquid–liquid–liquid equilibria were determined for (water + cyclohexylamine + toluene), (water + cyclohexylamine + propylbenzene), (water + cyclohexylamine + heptane), and (water + cyclohexylamine + octane) at temperatures of (298.15, 303.15, and 333.15) K at atmospheric pressure by photometric turbidity titration. The composition of conjugate phases was determined by gas–liquid chromatography or potentiometric titration and Karl Fischer titration. All systems show type I behavior since there is only one binary pair of partial miscible liquids. Surprisingly, the systems (water + cyclohexylamine + heptane) and (water + cyclohexylamine + octane) have a three-phase region in a limited temperature range. The data were predicted with the NRTL and the UNIQUAC models in comparison to the Elliott–Suresh–Donohue equation of state based on binary interaction parameters only.

## Introduction

For chemical engineering separation processes knowledge of the phase equilibrium is indispensable. The liquid–liquid equilibria (LLE) and liquid–liquid–liquid equilibria (LLLE) of mixtures are especially interesting for extraction processes. The investigations showed particular phase behavior. While the systems with the aromatic hydrocarbons (toluene and propylbenzene) showed normal type 1 phase behavior (classification of Treyball<sup>1</sup>), in the systems with aliphatic hydrocarbons (heptane and octane), three liquid phases occurred in a limited temperature range. This three-phase region was not expected since a miscibility gap exists in the binary system of hydrocarbon + water only. This characteristic arises from the structure of cyclohexylamine (CHA). It can provide polar (amine group) and nonpolar (cyclic CH<sub>2</sub> group) interactions. Since these interactions change strongly with temperature, the LL(L)E show interesting temperature dependences.

## Experimental Section

**Materials.** Heptane was obtained from Fisher Scientific Ltd., U.K., with a mass fraction purity > 99 %. Octane with purity > 99 %, cyclohexylamine purity p.a., and toluene purity p.a. were purchased from Acros Organics, Belgium. Propylbenzene with purity > 98 % was obtained from Merck KGaA, Germany. The purity was judged by comparing experimental values of refractive index and density with values reported in the literature (cf. Table 1). Additionally, the purity was verified by gas–liquid chromatography (GLC). The mass fractions of the substances are as follows: cyclohexylamine (99.9 %), toluene (99.8 %), propylbenzene (99.5 %), heptane (99.5 %), and octane (99.8 %). The substances were used as received since the purities determined by GLC are greater than 99.5 % each time. Distilled and deionized water was used.

\* Corresponding author. Tel.: +49-351-462-2777. Fax: +49-351-462-3228. E-mail: schmelzer@mw.htw-dresden.de.

**Table 1.** Comparison of Experimental Refractive Index,  $n_D$ , and Density,  $\rho$ , of Pure Liquids with Literature Values<sup>19</sup>

substance	T/K	$n_D$		$\rho$ (g·cm <sup>-3</sup> )	
		exptl	lit	exptl	lit
heptane	298.15	1.3853	1.3855	0.67943	0.6795
octane	298.15	1.3946	1.3944	0.69849	0.6986
toluene	293.15	1.4960	1.4961	0.86678	0.8668
propylbenzene	298.15	1.4901	1.4895	0.86079	0.8593
CHA	288.15	1.4624	1.4625		
	303.15			0.85820	0.85777 <sup>a</sup>
water	293.15	1.3336	1.3336	0.99816	0.9982

<sup>a</sup> Ref 20.

**Apparatus and Procedure.** The binodal curves were determined by photometric turbidity titration<sup>2</sup> (cp. Figure 1). A homogeneous mixture (for example, of hydrocarbon and cyclohexylamine) is filled into the tempered glass vessel. The masses of the components are determined by weighing (accuracy 0.5 mg). The temperature is held constant with a thermostat within a range of  $\pm 0.1$  K. The third component (in our case water) is added via an automatic buret (808 Titrande, Deutsche Metrohm, Filderstadt). The mixture is stirred, and for a faster dispensation of the dosed water drops and for a faster equilibration, an ultrasonic wave generator (UW 2070, BANDELIN

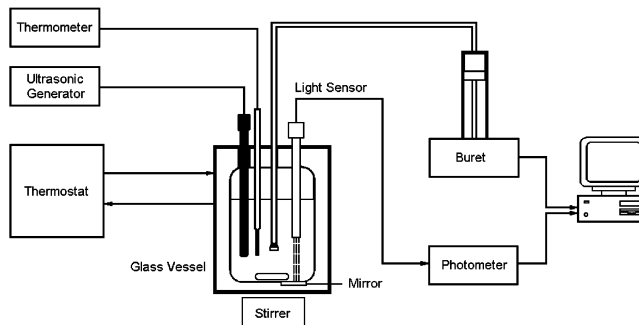


**Figure 1.** Scheme of photometric turbidity titration method.

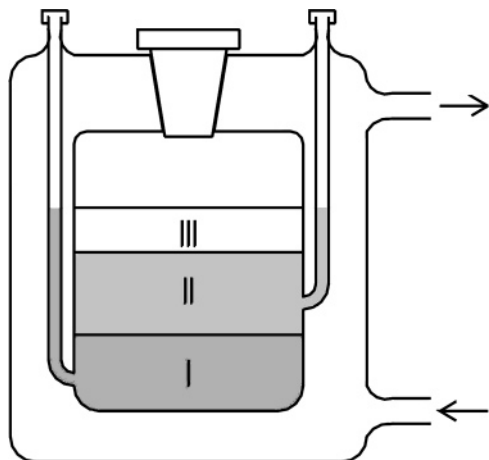


Figure 2. Glass vessel used for the measurements of LLE and LLE.

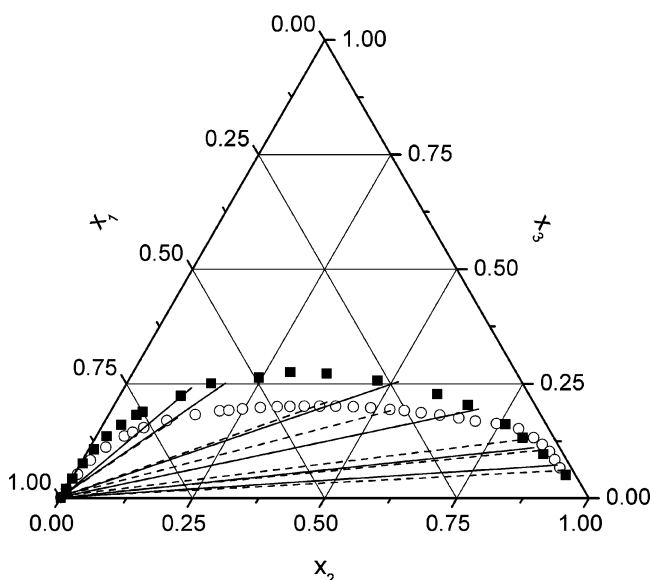


Figure 3. Experimental results in the water (1) + toluene (2) + CHA (3) system: O, experimental binodal curve at 298.15 K; ■, experimental binodal curve at 333.15 K; dashed line, tie lines at 298.15 K; solid line, tie lines at 333.15 K.

Electronic, Berlin) of low power is used. The solubility limit is obtained by measurement of the light transmission using the photometer 662 (Deutsche Metrohm, Filderstadt). The data are logged with a PC. An intensive turbidity indicates the occurrence of the two-phase region and a new point of the binodal curve. For a new measurement point, the dissolving component (cyclohexylamine) is added until the mixture is homogeneous again, and a new titration is progressed. For measurement of the other side of the binodal curve, the corresponding components must be interchanged. The equilibrium compositions of the liquid phases in ternary systems are determined with an average precision for the mole fraction of  $\pm 0.003$ .

The composition of the conjugate phases (tie lines and three-phase regions) is determined by the analytic method. Defined mixtures of the components are equilibrated in a temperature-regulated glass vessel with sample points at different heights (cp. Figure 2). Through these sample points, samples of each phase can be taken without piercing of other phases. The phases are equilibrated by intense stirring for 4 h. Afterward the phases are allowed to separate for at least 24 h, and samples of each phase are taken with syringes. The temperature is held constant within a range of  $\pm 0.1$  K. The systems water + toluene +

Table 2. LLE of the Water (1) + Toluene (2) + CHA (3) System at Atmospheric Pressure

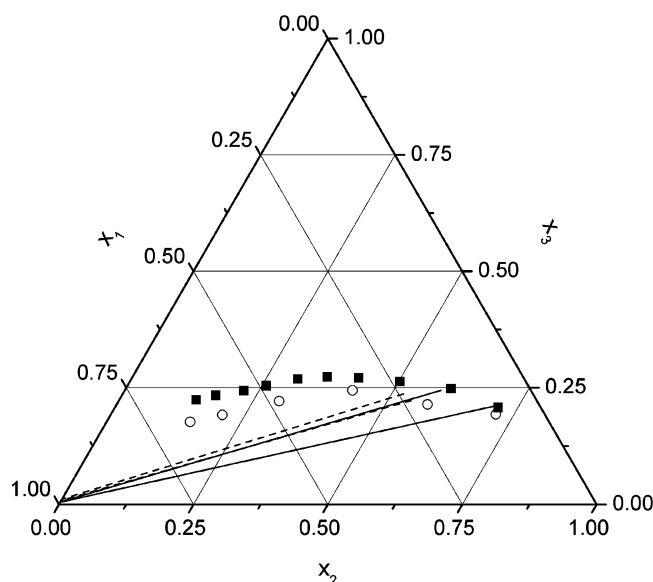
$T = 298.15$ K			$T = 333.15$ K		
$x_1$	$x_2$	$x_3$	$x_1$	$x_2$	$x_3$
0.9978	0.0003	0.0019	0.9984	0.0006	0.0010
0.9780	0.0018	0.0202	0.9784	0.0008	0.0208
0.9408	0.0069	0.0523	0.9553	0.0017	0.0430
0.9010	0.0154	0.0836	0.9187	0.0046	0.0767
0.8582	0.0303	0.1115	0.8825	0.0101	0.1074
0.8105	0.0532	0.1363	0.8443	0.0201	0.1356
0.7909	0.0646	0.1445	0.8045	0.0348	0.1607
0.7649	0.0808	0.1543	0.7653	0.0530	0.1817
0.7132	0.1169	0.1699	0.7500	0.0611	0.1889
0.6530	0.1639	0.1831	0.6600	0.1160	0.2240
0.6031	0.2059	0.1910	0.5888	0.1599	0.2513
0.5850	0.2229	0.1921	0.4924	0.2440	0.2636
0.5579	0.2469	0.1952	0.4267	0.2977	0.2756
0.5224	0.2793	0.1983	0.3598	0.3676	0.2726
0.4898	0.3100	0.2002	0.2711	0.4717	0.2572
0.4652	0.3340	0.2008	0.1730	0.5993	0.2277
0.4377	0.3612	0.2011	0.1268	0.6691	0.2041
0.4082	0.3904	0.2014	0.0773	0.7610	0.1617
0.3783	0.4207	0.2010	0.0590	0.8089	0.1321
0.3457	0.4543	0.2000	0.0383	0.8653	0.0964
0.3141	0.4885	0.1974	0.0180	0.9307	0.0513
0.2795	0.5265	0.1940			
0.2530	0.5552	0.1918			
0.2240	0.5890	0.1870			
0.1912	0.6273	0.1815			
0.1581	0.6660	0.1759			
0.1306	0.7007	0.1687			
0.0931	0.7433	0.1636			
0.0567	0.7913	0.1520			
0.0381	0.8293	0.1326			
0.0292	0.8532	0.1176			
0.0232	0.8746	0.1022			
0.0223	0.8929	0.0848			
0.0213	0.9116	0.0671			
		Tie Lines			
<i>a</i>	0.0163	0.9224	0.0613	0.0233	0.0727
<i>b</i>	0.9954	0.0018	0.0028	0.9979	0.0007
<i>a</i>	0.0421	0.8531	0.1048	0.0492	0.1107
<i>b</i>	0.9947	0.0024	0.0029	0.9980	0.0008
<i>a</i>	0.0689	0.8037	0.1274	0.1117	0.6939
<i>b</i>	0.9939	0.0008	0.0053	0.9946	0.0019
<i>a</i>	0.2805	0.5286	0.1909	0.2337	0.5121
<i>b</i>	0.9909	0.0025	0.0066	0.9937	0.0018
<i>a</i>	0.3904	0.3993	0.2103	0.5620	0.1865
<i>b</i>	0.9929	0.0021	0.0050	0.9936	0.0009
<i>a</i>	0.6910	0.1335	0.1755	0.6309	0.1275
<i>b</i>	0.9901	0.0024	0.0075	0.9935	0.0021

<sup>a</sup> Top phase. <sup>b</sup> Bottom phase.

CHA and water + octane + CHA were analyzed by the titration method; the systems water + propylbenzene + CHA and water + heptane + CHA were analyzed by the GLC method. In the GLC method, the content of organic components is determined on a HP 6890 series gas chromatograph, equipped with a flame ionization detector. The content of water is calculated by subtraction from unity. The determination of the organic components has an accuracy of  $\pm 0.005$  in mole fraction. In the titration method, CHA is determined by potentiometric titration with hydrochloric acid (0.1 mol/L) with a 716 DMS Titrino (Deutsche Metrohm, Filderstadt). Water is titrated according to the Karl Fischer method with a 787 KF Titrino (Deutsche Metrohm, Filderstadt). The content of the hydrocarbon is calculated by subtraction from unity. The potentiometric titration has an accuracy in mass fraction of 0.005, the Karl Fischer titration of 1 % of the measured mass fraction. In the systems with the aromatic hydrocarbons, the water-rich phase consists of almost pure water (the mole fraction is at least 0.99). This leads to analytical problems for both methods and to greater deviations of the composition (up to a mole fraction of 0.01) in the water-rich phase. Measurements of the binodal curve and

**Table 3. LLE of the Water (1) + Propylbenzene (2) + CHA (3) System at Atmospheric Pressure**

	$T = 303.15 \text{ K}$			$T = 333.15 \text{ K}$		
	$x_1$	$x_2$	$x_3$	$x_1$	$x_2$	$x_3$
	0.0908	0.7163	0.1929	0.0792	0.7129	0.2079
	0.2073	0.5788	0.2139	0.1470	0.6050	0.2480
	0.3316	0.4239	0.2445	0.2338	0.5028	0.2634
	0.4796	0.2992	0.2212	0.3074	0.4218	0.2708
	0.6001	0.2082	0.1917	0.3661	0.3612	0.2727
	0.6677	0.1553	0.1770	0.4216	0.3099	0.2685
				0.4876	0.2583	0.2541
				0.5345	0.2216	0.2439
				0.5913	0.1751	0.2336
				0.6326	0.1433	0.2241
			Tie Lines			
<i>a</i>	0.2339	0.5434	0.2227	0.1676	0.5879	0.2445
<i>b</i>	0.9907	0.0006	0.0087	0.9933	0.0008	0.0059
<i>a</i>	0.2413	0.5219	0.2368	0.0720	0.7144	0.2136
<i>b</i>	0.9876	0.0011	0.0113	0.9941	0.0006	0.0053

*a* Top phase. *b* Bottom phase.**Figure 4.** Experimental results in the water (1) + propylbenzene (2) + CHA (3) system: ○, experimental binodal curve at 303.15 K; ■, experimental binodal curve at 333.15 K; dashed line, tie lines at 303.15 K; solid line, tie lines at 333.15 K.

compositions of conjugate phases show good agreements in our investigations.

## Results

The binary mixtures of water + CHA and hydrocarbon + CHA are homogeneous over the whole concentration and temperature range. The binary mixtures of hydrocarbon + water were investigated by Tsionopoulos<sup>3,4</sup> and show a large miscibility gap. The solubility of water in the hydrocarbon phase rises with increasing temperature. The immiscibility of aromatic and aliphatic hydrocarbon in water has a maximum at around 291 K and 303 K, respectively. After this, the solubility also increases with increasing temperature.

**Water + Toluene + Cyclohexylamine.** The experimental results are listed in Table 2 and shown in Figure 3. The binodal curves and tie lines were measured at temperatures of 298.15 K and 333.15 K. The binodal curves have a flat pathway. The analysis of the tie lines shows that CHA is distributed almost completely in the toluene-rich phase. The water-rich phase consists nearly of pure water (minimum mole fraction of water

**Table 4. LLE of the Water (1) + Heptane (2) + CHA (3) System at Atmospheric Pressure**

	$T = 298.15 \text{ K}$			$T = 333.15 \text{ K}$		
	$x_1$	$x_2$	$x_3$	$x_1$	$x_2$	$x_3$
	0.9674	0.0024	0.0302	0.9458	0.0018	0.0524
	0.9479	0.0047	0.0474	0.9177	0.0055	0.0768
	0.9377	0.0062	0.0561	0.8459	0.0256	0.1285
	0.9211	0.0086	0.0703	0.7555	0.0625	0.1820
	0.8795	0.0157	0.1048	0.6883	0.0980	0.2137
	0.8502	0.0211	0.1287	0.6223	0.1413	0.2364
	0.8197	0.0278	0.1525	0.5177	0.2320	0.2503
	0.7060	0.0660	0.2280	0.4244	0.3208	0.2548
	0.6597	0.0915	0.2488	0.3342	0.4134	0.2524
	0.5462	0.1796	0.2742	0.2599	0.4899	0.2502
	0.4430	0.2884	0.2686	0.2072	0.5459	0.2469
	0.3969	0.3456	0.2575	0.1453	0.6153	0.2394
	0.3723	0.3737	0.2540	0.0717	0.7087	0.2196
	0.3541	0.3976	0.2483	0.0354	0.7767	0.1879
	0.3363	0.4224	0.2413	0.0193	0.8426	0.1381
	0.3142	0.4497	0.2361	0.0049	0.9548	0.0403
	0.2903	0.4790	0.2307			
	0.2672	0.5078	0.2250			
	0.2417	0.5398	0.2185			
	0.2142	0.5750	0.2108			
	0.1806	0.6180	0.2014			
	0.1547	0.6522	0.1931			
	0.1180	0.7013	0.1807			
	0.0705	0.7690	0.1605			
	0.0651	0.7772	0.1577			
	0.0556	0.7914	0.1530			
	0.0391	0.8142	0.1467			
	0.0169	0.8672	0.1159			
			Tie Lines			
<i>a</i>	0.0053	0.8982	0.0965	0.1114	0.6500	0.2386
<i>b</i>	0.9808	0.0001	0.0191	0.7249	0.0722	0.2029
<i>a</i>	0.0116	0.8730	0.1154	0.0058	0.8852	0.1090
<i>b</i>	0.7844	0.0355	0.1801	0.9965	0.0000	0.0035
<i>a</i>	0.0075	0.8950	0.0975			
<i>b</i>	0.8826	0.0135	0.1039			
<i>a</i>	0.0129	0.8700	0.1171			
<i>b</i>	0.7409	0.0526	0.2065			
<i>a</i>	0.0408	0.8080	0.1512			
<i>b</i>	0.6285	0.1079	0.2636			

*a* Top phase. *b* Bottom phase.**Table 5. Experimental Three-Phase Region in the System Water (1) + Heptane (2) + CHA (3) at Atmospheric Pressure**

$T/\text{K}$	top phase			middle phase			bottom phase		
	$x_1$	$x_2$	$x_3$	$x_1$	$x_2$	$x_3$	$x_1$	$x_2$	$x_3$
323.15	0.0332	0.7894	0.1774	0.8895	0.0139	0.0966	0.9833	0.0083	0.0084
333.15	0.0782	0.7047	0.2171	0.8435	0.0296	0.1269	0.9958	0.0006	0.0036
343.15	0.2342	0.4924	0.2734	0.7190	0.0768	0.2042	0.9929	0.0008	0.0063

is 0.99). The ternary two-phase region becomes larger with increasing temperature from 298.15 K to 333.15 K in the toluene system. The plait point is located very asymmetrically close to the high water concentrations.

**Water + Propylbenzene + Cyclohexylamine.** The results are presented in Table 3 and Figure 4. The experimental results are similar to the results in the toluene system; therefore, only fewer points were recorded. The LLE were investigated at 303.15 K and 333.15 K. The temperature dependence of the ternary miscibility gap is less distinct than in the toluene system but has the same tendency. The tie lines and the plait point are also strongly asymmetrical because CHA is accumulated in the propylbenzene-rich phase.

**Water + Heptane + Cyclohexylamine.** The experimental results are summarized in Tables 4 and 5 and in Figures 5 and 6. The binodal curves and tie lines were measured at 298.15 K

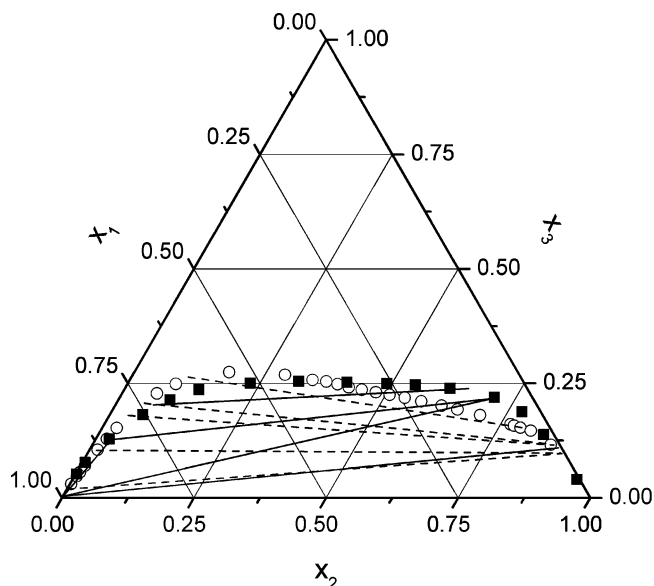


**Figure 5.** Experimental results in the water (1) + heptane (2) + CHA (3) system: ○, experimental binodal curve at 298.15 K; ■, experimental binodal curve at 333.15 K; dashed line, tie lines at 298.15 K; solid line, tie lines and three-phase region at 333.15 K.

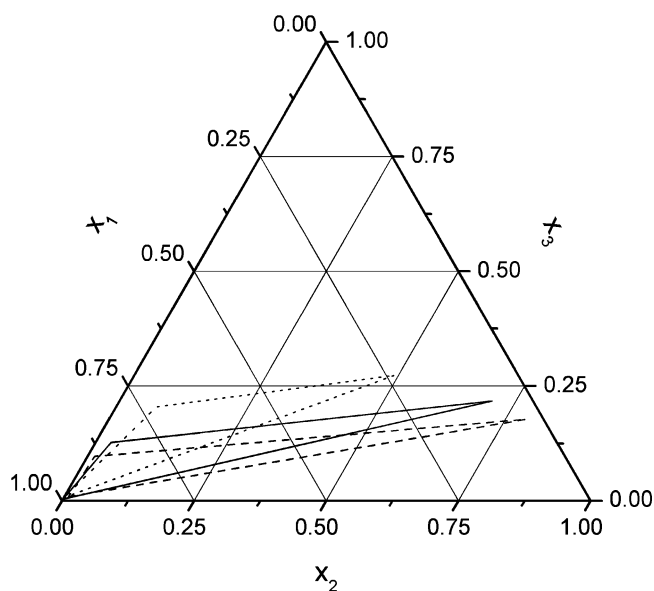


**Figure 6.** Temperature dependence of the three-phase region in the water (1) + heptane (2) + CHA (3) system: dashed line, 323.15 K; solid line, 333.15 K; dotted line, 343.15 K.

and 333.15 K. The compositions of the three-phase region were determined at 323.15 K, 333.15 K, and 343.15 K. The binodal curves have a flat pathway. A very interesting characteristic is the inversion of the slope of the binodal curves from 298.15 K to 333.15 K. The change of temperature has almost no influence on the size of the miscibility gap. The measured tie lines at 298.15 K converge in a region of high heptane concentration, so this system shows solutropy.<sup>5</sup> In the temperature range of 318.15 K to 345.15 K, the occurrence of a three-phase region was observed. The three-phase region shifts to higher CHA concentrations with rising temperatures.

**Water + Octane + Cyclohexylamine.** The experimental results are listed in Tables 6 and 7 and pictured in Figures 7 and 8. For the experimental results, the same statements as for the heptane system are generally valid. The binodal curves at

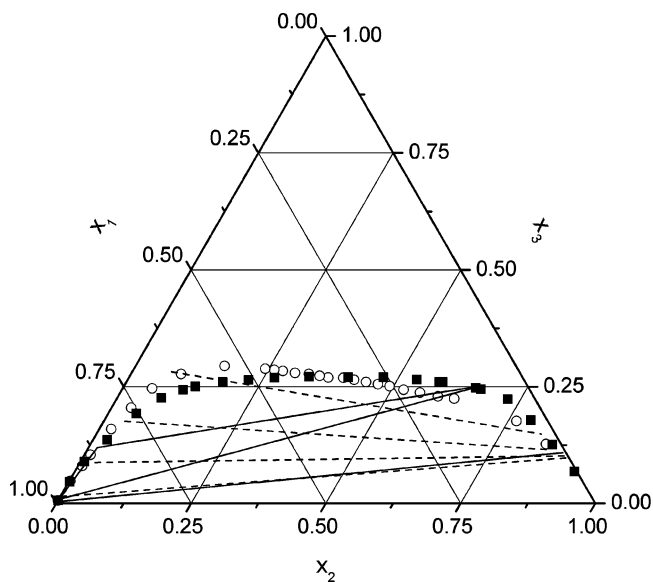


**Figure 7.** Experimental results in the water (1) + octane (2) + CHA (3) system: ○, experimental binodal curve at 298.15 K; ■, experimental binodal curve at 333.15 K; dashed line, tie lines at 298.15 K; solid lines, tie lines and three-phase region at 333.15 K.

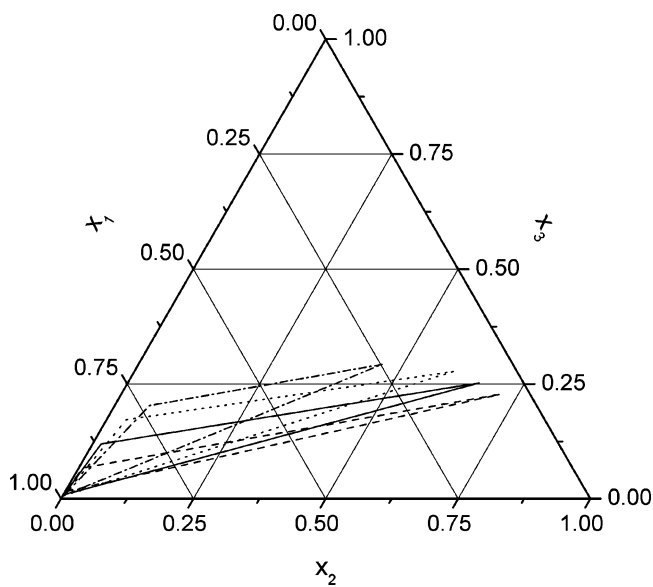


**Figure 8.** Temperature dependence of the three-phase region in the water (1) + octane (2) + CHA (3) system: dashed line, 323.15 K; solid line, 333.15 K; dotted line, 343.15 K; dash-dotted line, 345.35 K.

298.15 K and 333.15 K intersect each other, and a three-phase region was observed in the temperature range from 313.15 K to 345.35 K. At 298.15 K the system shows solutropy.

## Calculations

**Correlation of Binary Data.** The experimental data in the binary systems were correlated using the Gibbs excess energy models UNIQUAC<sup>6</sup> and NRTL<sup>7</sup> and the equation of state proposed by Elliott, Suresh, and Donohue<sup>8,9</sup> (ESD EoS). The binary interaction parameters of the activity coefficient models were assumed to be temperature dependent (eq 1):

$$C_{ij}/R = C_{ij}^C + C_{ij}^T(T - 273.15 \text{ K}) \quad (1)$$

where  $C_{ij} = u_{ij} - u_{ji}$  for UNIQUAC and  $C_{ij} = g_{ij} - g_{ji}$  for

**Table 6. LLE of the Water (1) + Octane (2) + CHA (3) System at Atmospheric Pressure**

T = 298.15 K			T = 333.15 K		
x <sub>1</sub>	x <sub>2</sub>	x <sub>3</sub>	x <sub>1</sub>	x <sub>2</sub>	x <sub>3</sub>
0.9940	0.0001	0.0059	0.9938	0.0004	0.0058
0.9498	0.0023	0.0479	0.9520	0.0020	0.0460
0.9116	0.0076	0.0808	0.9025	0.0080	0.0895
0.8840	0.0116	0.1044	0.8370	0.0266	0.1364
0.8184	0.0224	0.1592	0.7550	0.0520	0.1930
0.7584	0.0369	0.2047	0.6922	0.0821	0.2257
0.6991	0.0546	0.2463	0.6429	0.1136	0.2435
0.6296	0.0935	0.2769	0.6167	0.1327	0.2506
0.5403	0.1654	0.2943	0.5614	0.1788	0.2598
0.4684	0.2434	0.2882	0.5109	0.2248	0.2643
0.4525	0.2615	0.2860	0.4606	0.2706	0.2688
0.4376	0.2789	0.2835	0.3954	0.3333	0.2713
0.4171	0.3032	0.2797	0.3236	0.4062	0.2702
0.3929	0.3299	0.2772	0.2578	0.4724	0.2698
0.3749	0.3520	0.2731	0.1981	0.5364	0.2655
0.3608	0.3696	0.2696	0.1588	0.5807	0.2605
0.3325	0.3985	0.2690	0.1530	0.5873	0.2597
0.3150	0.4205	0.2645	0.0977	0.6550	0.2473
0.2952	0.4447	0.2601	0.0902	0.6653	0.2445
0.2755	0.4694	0.2551	0.0503	0.7263	0.2234
0.2559	0.4932	0.2509	0.0306	0.7913	0.1781
0.2335	0.5232	0.2433	0.0163	0.8575	0.1262
0.2063	0.5562	0.2375	0.0046	0.9265	0.0689
0.1770	0.5938	0.2292			
0.1493	0.6265	0.2242			
0.0578	0.7659	0.1763			
0.0274	0.8450	0.1276			
Tie Lines					
a	0.0254	0.8257	0.1489	0.0055	0.1090
b	0.6452	0.0730	0.2818	0.9960	0.0038
a	0.0317	0.8530	0.1153		
b	0.7849	0.0391	0.1760		
a	0.0068	0.8913	0.1019		
b	0.9023	0.0100	0.0877		
a	0.0061	0.8962	0.0977		
b	0.9835	0.0016	0.0149		

<sup>a</sup> Top phase. <sup>b</sup> Bottom phase.

**Table 7. Experimental Three-Phase Region in the System Water (1) + Octane (2) + CHA (3) at Atmospheric Pressure**

T/K	top phase			middle phase			bottom phase		
	x <sub>1</sub>	x <sub>2</sub>	x <sub>3</sub>	x <sub>1</sub>	x <sub>2</sub>	x <sub>3</sub>	x <sub>1</sub>	x <sub>2</sub>	x <sub>3</sub>
323.15	0.0578	0.7150	0.2272	0.9252	0.0075	0.0673	0.9829	0.0010	0.0161
333.15	0.0842	0.6638	0.2520	0.8646	0.0160	0.1194	0.9900	0.0010	0.0090
343.15	0.1209	0.6022	0.2769	0.7906	0.0372	0.1722	0.9928	0.0010	0.0062
345.35	0.2473	0.4601	0.2926	0.7312	0.0659	0.2029	0.9900	0.0021	0.0079

NRTL. The objective function of Renon et al.<sup>10</sup> was used:

$$Q = \Pi_1 \sum_i \left( \frac{100}{P_{\text{expt}/i}} \right)^2 (P_{\text{calcd}} - P_{\text{expt}/i})^2 + \Pi_2 \sum_i (100)_i^2 (y_{1,\text{calcd}} - y_{1,\text{expt}/i})^2 + \Pi_3 \sum_i (100)_i^2 (x'_{1,\text{calcd}} - x'_{1,\text{expt}/i})^2 + \Pi_4 \sum_i (100)_i^2 (x''_{1,\text{calcd}} - x''_{1,\text{expt}/i})^2 \quad (2)$$

where  $P$  is the pressure,  $y$  is the vapor phase mole fraction,  $x'$  and  $x''$  are the mole fractions of the different phases at liquid–liquid equilibrium and  $\Pi_i$  is a weighting factor. The binary ESD EoS parameters  $k_{ij}$  were also assumed to depend on temperature (eq 3):

$$k_{ij} = k_{ij}^C + k_{ij}^T (T - 273.15 \text{ K}) \quad (3)$$

The pure component parameters for the ESD EoS are listed in Table 8. Pure component parameters for CHA were not available; therefore, new parameters were fitted to vapor pressure data and volumes of saturated liquid from the DIPPR

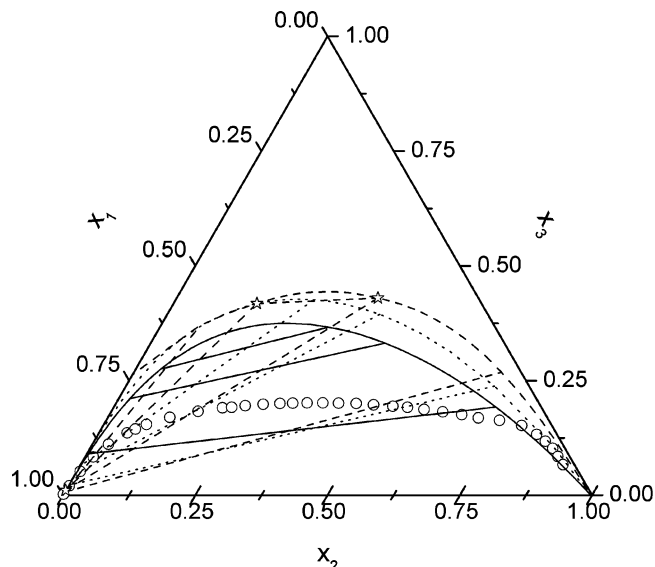


**Figure 9.** Results of prediction in the water (1) + toluene (2) + CHA (3) system at 298.15 K: ○, experimental binodal curve; dotted line, UNIQAC model; dashed line, NRTL model; solid line, ESD EoS; ☆, indicates vertexes of a three-phase region.

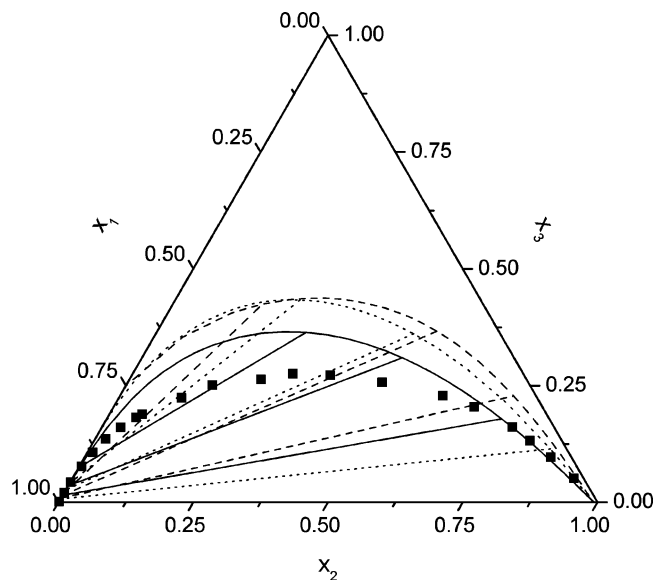


**Figure 10.** Results of prediction in the water (1) + toluene (2) + CHA (3) system at 333.15 K: ■, experimental binodal curve; dotted line, UNIQAC model; dashed line, NRTL model; solid line, ESD EoS.

correlations.<sup>11</sup> The specified quality code is less than 5 % for the vapor pressure correlation and less than 3 % for the density correlation.

The used data sets, parameters, and deviations of binary fits are summarized in Tables 9, 10, and 11. The binary data of Zlacký et al.<sup>12</sup> for the system toluene + CHA were omitted since they do not pass the consistency test of Christiansen and Fredenslund<sup>13</sup> with the consistency criterion of Danner and Gess.<sup>14</sup> Phase equilibrium data for the systems propylbenzene + CHA and heptane + CHA are not available. For this reason, VLE data at 333.15 K and 363.15 K were predicted with the Modified UNIFAC model (Dortmund).<sup>15</sup>

**Prediction of Ternary Phase Behavior.** In all ternary systems, the calculated miscibility gap is too large. For the binary system of water + CHA, a miscibility gap is calculated with the NRTL model at high water concentrations. However, this system is



**Table 8. Pure Component Parameters for the ESD EoS**

substance	water	CHA	toluene	propylbenzene	heptane	octane
reference	21	this work <sup>a</sup>	21	21	21	21
$\epsilon_i/k/K$	427.25	460.27	332.75	332.53	280.69	285.211
$v_i^*/(10^{23}\cdot\text{cm}^3\cdot\text{mol}^{-1})$	9.411	45.806	44.238	48.326	47.761	54.157
$c$	1.0053	1.1090	1.9707	2.2877	2.3002	2.2842
$\epsilon_{\text{HB}}/RT_{\text{crit}}$	4.0000	3.320				
$K_{\text{AB}}/v_i^*$	0.1000	0.0621				

<sup>a</sup>  $T_r = 0.47-0.90$ ; weighting of  $P^{\text{sat}} = 1$ ; weighting of  $v^{\text{liq}} = 1$ ;  $\Delta P^{\text{sat}} = 1.32\%$ ;  $\Delta v^{\text{liq}} = 1.28\%$ .

**Table 9. Parameters and Results of the Binary Systems for the NRTL Model**

system	reference	$C_{12}^C/K$	$C_{21}^C/K$	$C_{12}^T$	$C_{21}^T$	$\alpha$	$\Delta P/\%$	$\Delta y$	$\Delta x$
water (1) + CHA (2)	16, 17, 18	1186.17	-13.11			0.47	1.83	0.0187	
toluene (1) + CHA (2)	22	167.80	-69.09	0.4729	-0.5633	0.47	0.31	0.0110	
water (1) + toluene (2)	4, 23, 24	1983.05	1397.47	6.0602	-5.3412	0.20	2.58	0.0146	0.000076
propylbenzene (1) + CHA (2)	UNIFAC prediction	-47.41	9.82	7.2756	-3.5860	0.47	0.54	0.0043	
water (1) + propylbenzene (2)	4	3869.87	1676.37	-5.1767	-6.4534	0.20			0.000006
heptane (1) + CHA (2)	UNIFAC prediction	23.86	278.26	2.5628	-3.5481	0.47	0.089	0.00059	
water (1) + heptane (2)	3, 25, 26	3497.63	2028.97	10.4226	-5.6490	0.20	4.11	0.0276	0.000094
octane (1) + CHA (2)	16	135.08	112.31			0.47	1.03	0.0059	
water (1) + octane (2)	3, 25	3260.80	2141.80	12.5591	-7.5243	0.20	2.67	0.0169	0.000040

**Table 10. Parameters and Results of the Binary Systems for the UNIQUAC Model**

system	reference	$C_{12}^C/K$	$C_{21}^C/K$	$C_{12}^T$	$C_{21}^T$	$\Delta P/\%$	$\Delta y$	$\Delta x$
water (1) + CHA (2)	16, 17, 18	30.03	-13.51	-0.1823	0.8887	2.06	0.0185	
toluene (1) + CHA (2)	22	68.94	-43.92	0.7689	-0.6611	0.30	0.0111	
water (1) + toluene (2)	4, 23, 24	311.50	1016.32	0.8284	-3.6809	2.74	0.0145	0.000068
propylbenzene (1) + CHA (2)	UNIFAC prediction	16.20	-41.73	4.3335	-2.3660	0.52	0.0042	
water (1) + propylbenzene (2)	4	302.40	1098.43	1.1130	-3.3503			0.000004
heptane (1) + CHA (2)	UNIFAC prediction	4.84	43.87	2.3556	-1.9660	0.076	0.00053	
water (1) + heptane (2)	3, 25, 26	525.20	1398.94	1.7004	-4.1248	4.16	0.0279	0.000099
octane (1) + CHA (2)	16	107.52	-44.05			1.13	0.0067	
water (1) + octane (2)	3, 25	381.79	1558.09	1.8703	-5.8408	2.71	0.0168	0.000042

**Table 11. Parameters and Results of the Binary Systems for the ESD EoS**

system	reference	$k_{ij}^C$	$k_{ij}^T/K^{-1}$	$\Delta P/\%$	$\Delta y$	$\Delta x$
water (1) + CHA (2)	16, 17, 18	-0.005326	0.00084086	2.29	0.0141	
toluene (1) + CHA (2)	22	-0.019579	0.00012097	1.12	0.0169	
water (1) + toluene (2)	4, 23, 24	0.078281	0.00056063	11.29	0.0663	0.000576
propylbenzene (1) + CHA (2)	UNIFAC prediction	-0.019745	0.00004335	1.19	0.0107	
water (1) + propylbenzene (2)	4	0.078642	0.00069182			0.000048
heptane (1) + CHA (2)	UNIFAC prediction	-0.003855	-0.00000865	1.51	0.0086	
water (1) + heptane (2)	3, 25, 26	0.134979	0.00093568	5.20	0.0563	0.000303
octane (1) + CHA (2)	16	-0.003042		1.46	0.0154	
water (1) + octane (2)	3, 25	0.154728	0.00066375	5.97	0.0176	0.000269

homogeneous over the whole concentration range, but the VLE data<sup>16-18</sup> show a homogeneous maximum azeotrope at high water concentrations. Further calculations showed that the miscibility gap disappears if an  $\alpha$  value above 1.1 is chosen, but then the deviations of the binary fit increase rapidly. Therefore, the parameter set with  $\alpha = 0.47$  was used.

In the water + toluene + CHA system (cp. Figures 9 and 10), the activity coefficient models and the ESD EoS yield similar results at 333.15 K. The slope of the predicted tie lines is in accord with the experimental results. However, at 298.15 K the ESD EoS and the NRTL model have substantial difficulties. The NRTL model predicts a three-phase region and the ESD EoS predicts almost parallel arranged tie lines, converse to the experimental results. Only the UNIQUAC model predicts tie lines that are adequate to the experimental results. The temperature dependence of the miscibility gap is not considered correctly in all predictions.

In the system water + propylbenzene + CHA, the prediction of the binodal curve from all correlations is similar for both temperatures but misses the experimental results. On account of this, only the results at 303.15 K are presented in Figure 11.

The slope of the tie lines is predicted well by the activity coefficient models. The ESD EoS gives worse results and delivers an almost parallel location of the tie lines.

The results for the system water + heptane + CHA are diagrammed in Figures 12 and 13. The predictions for the LLE at 298.15 K do not match the experimental results. None of the predictions reports the particular pathway of the tie lines at 298.15 K. The NRTL model predicts a three-phase region, and the UNIQUAC model and the ESD EoS predict parallel tie lines. At 333.15 K, the UNIQUAC model forecasts a three-phase region, but the location of the three-phase region is not rendered well. Accordingly, the prediction of the tie lines is not in good agreement with the experimental results. With the ESD EoS, parallel tie lines are calculated over the whole immiscible region. The NRTL model predicts tie lines ending up almost in pure water, similar to the results with the aromatic hydrocarbons.

The results for the water + octane + CHA system are shown in Figure 14. The predictions are similar to the heptane system; therefore, only the results at 333.15 K are presented. At 298.15 K, the UNIQUAC model and the ESD EoS forecast almost parallel tie lines while the NRTL model predicts a three-phase

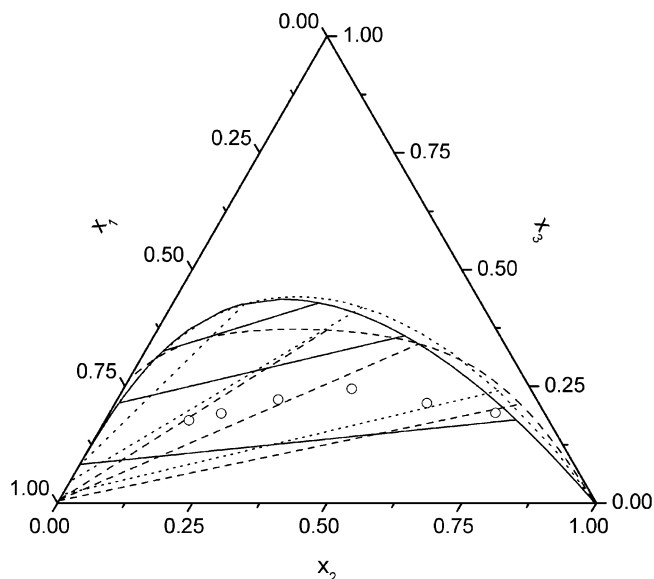


**Figure 11.** Results of prediction in the water (1) + propylbenzene (2) + CHA (3) system at 303.15 K: ○, experimental binodal curve; dotted line, UNIQUAC model; dashed line, NRTL model; solid line, ESD EoS.

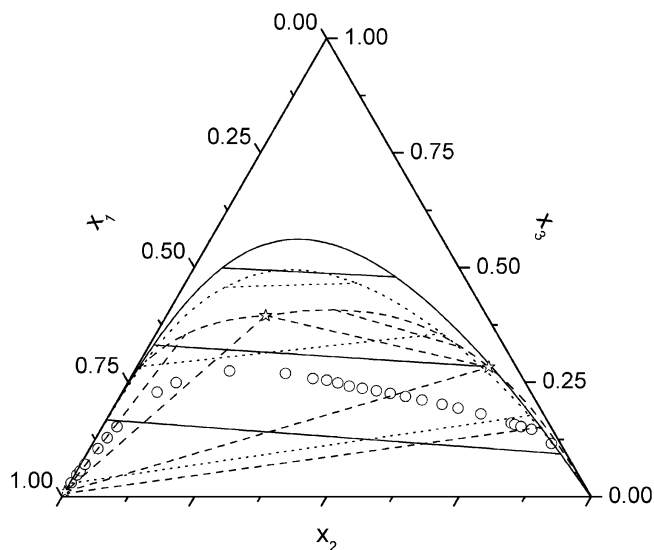


**Figure 12.** Results of prediction in the water (1) + heptane (2) + CHA (3) system at 298.15 K: ○, experimental binodal curve; dotted line, UNIQUAC model; dashed line, NRTL model; solid line, ESD EoS; ☆, indicates vertexes of a three-phase region.

region. At 333.15 K, the UNIQUAC model predicts a three-phase region whose composition does not agree with experimental results. The ESD EoS and the NRTL model predict similar to the heptane system parallel tie lines and tie lines ending up in almost pure water, respectively.

The ternary prediction of the toluene and the propylbenzene system leads to similar results as in the heptane and the octane system. This admits the conclusion that the predictions of binary data in the system cyclohexylamine + propylbenzene or heptane with the Modified UNIFAC model (Dortmund) is possible.

## Conclusions

The LLE for the ternary systems water + cyclohexylamine + toluene, + propylbenzene, + heptane, or + octane were determined (tie lines and binodal curve) at atmospheric pressure for two temperatures. The different experimental methods show good agreement. The predictions outgoing from binary model parameters based on vapor–liquid equilibria and LLE data show

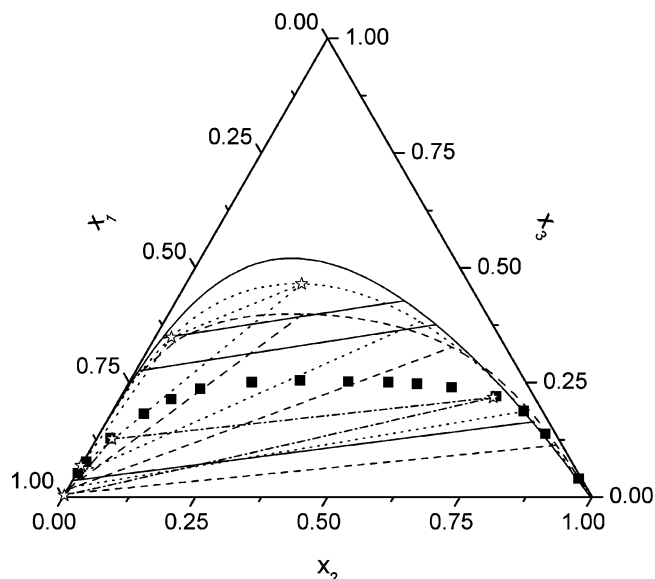


**Figure 13.** Results of prediction in the water (1) + heptane (2) + CHA (3) system at 333.15 K: ■, experimental binodal curve; dash-dotted line, experimental three-phase region; dotted line, UNIQUAC model; dashed line, NRTL model; solid line, ESD EoS; ☆, indicates vertexes of a three-phase region.

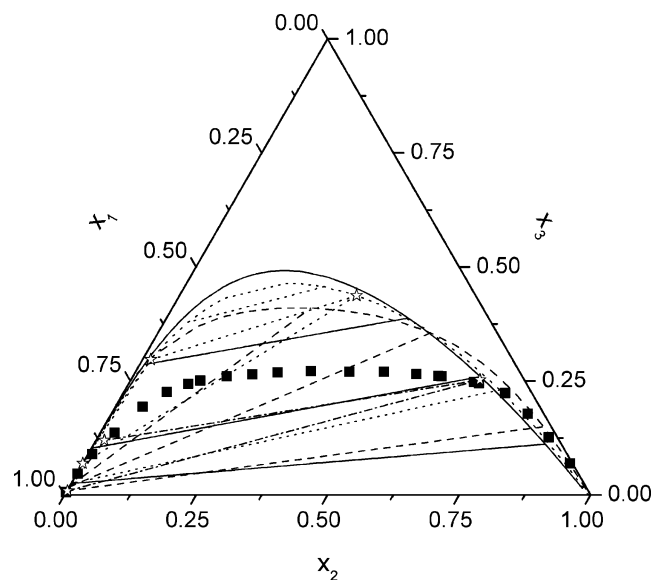


**Figure 14.** Results of prediction in the water (1) + octane (2) + CHA (3) system at 333.15 K: ■, experimental binodal curve; dash-dotted line, experimental three-phase region; dotted line, UNIQUAC model; dashed line, NRTL model; solid line, ESD EoS; ☆, indicates vertexes of a three-phase region.

large deviations from the experimental results for the NRTL and UNIQUAC model and for the ESD EoS.

## Acknowledgment

The authors are very grateful to Roland Schumann, Rainer Bitterlich, Jörg Arnold, and Kristina Lehmann for technical assistance.

## Literature Cited

- (1) Treybal, R. E. *Liquid Extraction*; McGraw-Hill: New York, 1963.
- (2) Schmelzer, J.; Taubert, K.; Martin, A.; Meinhardt, R.; Kempe, J. Phase equilibria in ternary systems containing phenols, hydrocarbons, and water. In *Thermodynamic Properties of Complex Fluid Mixtures*; Maurer, G., Ed.; Wiley-VCH: Weinheim, Germany, 2004; pp 135–149.

- (3) Tsonopoulos, C. Thermodynamic analysis of the mutual solubilities of normal alkanes and water. *Fluid Phase Equilib.* **1999**, *156*, 21–33.
- (4) Tsonopoulos, C. Thermodynamic analysis of the mutual solubilities of hydrocarbons and water. *Fluid Phase Equilib.* **2001**, *186*, 185–206.
- (5) Smith, A. S. Solutropes. *Ind. Eng. Chem.* **1950**, *42*, 1206–1209.
- (6) Abrams, D. S.; Prausnitz, J. M. Statistical thermodynamics of liquid mixtures: a new expression for the excess Gibbs energy of partly or completely miscible systems. *AIChE J.* **1975**, *21*, 116–128.
- (7) Renon, H.; Prausnitz, J. M. Local compositions in thermodynamic excess functions for liquid mixtures. *AIChE J.* **1968**, *14*, 135–144.
- (8) Elliott, J. R.; Suresh, S. J.; Donohue, M. D. A simple equation of state for non-spherical and associating molecules. *Ind. Eng. Chem. Res.* **1990**, *29*, 1476–1485.
- (9) Suresh, S. J.; Elliott, J. R. Multiphase equilibrium analysis via a generalized equation of state for associating mixtures. *Ind. Eng. Chem. Res.* **1992**, *31*, 2783–2794.
- (10) Renon, H.; Asselineau, L.; Cohen, G.; Raimbault, C. *Calcul sur ordinateur des équilibres liquide-vapeur et liquide-liquide*; Editions Technip: Paris, 1971.
- (11) Daubert, T. E.; Danner, R. P. *Physical and Thermodynamic Properties of Pure Chemicals: Data Compilation*; Hemisphere: New York, 2003.
- (12) Zlácký, A.; Hyška, K.; Mičudová, J. Rovnovaha kvapalina–para binarných zmesí *n*-butanol–cyclohexylamin a toluen–cyclohexylamin (Liquid–vapor equilibrium of binary *n*-butanol–cyclohexylamine and toluene–cyclohexylamine mixtures). *Petrochemia* **1990**, *30*, 150–153.
- (13) Christiansen, L. J.; Fredenslund, A. Thermodynamic consistency using orthogonal collocation or computation of equilibrium vapor compositions at high pressures. *AIChE J.* **1975**, *21*, 49–57.
- (14) Danner R. P.; Gess, M. A. A data base standard for the evaluation of vapor–liquid–equilibrium models. *Fluid Phase Equilib.* **1990**, *56*, 285–301.
- (15) Weidlich, U.; Gmehling, J. A modified UNIFAC model. 1. Prediction of VLE,  $h^E$ , and  $\gamma^\infty$ . *Ind. Eng. Chem. Res.* **1987**, *26*, 1372–1381.
- (16) Grenner, A.; Klauck, M.; Schmelzer, J. An equipment for dynamic measurement of vapour–liquid equilibria and results in binary systems containing cyclohexylamine. *Fluid Phase Equilib.* **2005**, *233*, 170–175.
- (17) Tanaka, H.; Kodama, D.; Yaginuma, R.; Kato, M. Vapor–liquid equilibria of aqueous solutions containing 2-aminoethanol or cyclohexylamine. *Netsu Bussei* **2001**, *15*, 182–184.
- (18) Carswell, T. S.; Morrill, H. L. Cyclohexylamine and dicyclohexylamine properties and uses. *Ind. Eng. Chem.* **1937**, *29*, 1247–1251.
- (19) Lide, D. R.; Frederike, H. P. R. *CRC Handbook of Chemistry and Physics on CD-ROM*; CRC Press: Boca Raton, FL, 2004.
- (20) Timmermans, J. *Physico-Chemical Constants of Pure Organic Compound*, Vol. 2, 2nd ed.; Elsevier: New York, 1965.
- (21) Elliott, J. R.; Lira, C. T. <http://www.egr.msu.edu/~lira/readcomp.htm> (esdparms.txt from progpack.exe; accessed December 2005).
- (22) Grenner, A.; Klauck, M.; Kramer, M.; Schmelzer, J. Activity coefficients at infinite dilution of cyclohexylamine + octane, toluene, ethylbenzene, or aniline and excess molar volumes in binary mixtures of cyclohexylamine + heptane, octane, nonane, decane, undecane, aniline, or water. *J. Chem. Eng. Data* **2006**, *51*, 176–180.
- (23) Omoto, T.; Esaki, M. Rapid determination of vapor–liquid equilibria by dynamic distillation Method. *Kagaku Kagaku (Abridged ed.)* **1967**, *5*, 36–38.
- (24) Jou, F.-Y.; Mather, A. E. Liquid–liquid equilibria for binary mixtures of water + benzene, water + toluene, and water + *p*-xylene from 273 K to 458 K. *J. Chem. Eng. Data* **2003**, *48*, 750–752.
- (25) Gmehling, J.; Menke, J.; Krafczyk, J.; Fischer, K. *Azeotropic Data. Part II*; Wiley-VCH: Weinheim, Germany, 1994.
- (26) Rezanova, E. N.; Toikka, A. M.; Markuzin, N. P. Equilibrium of two and three liquid phases with vapor in the *n*-heptane–nitromethane–water system. I. Experimental data. *Vestn. Leningr. Univ., Fiz. Khim.* **1991**, *4* (18), 53–56.

Received for review December 13, 2005. Accepted February 22, 2006.  
The authors gratefully acknowledge the grant for M.K. of the Saxon  
Ministry of Science and the Fine Arts.

JE050520F